www.czasopisma.pan.pl PAN www.journals.pan.pl

ARCHIVES of FOUNDRY ENGINEERING

ISSN (2299-2944)
Volume 2020
Issue 2/2020

118 – 122

10.24425/afe.2020.131313

20/2

Published quarterly as the organ of the Foundry Commission of the Polish Academy of Sciences

Preparation and Microstructure Evolution of Continuous Unidirectional Solidification Tin Bronze Alloy at Different Continuous Casting Speed

Jihui Luo
College of Materials Science and Engineering,
Yangtze Normal University, China
Corresponding author. E-mail: 20170128@yznu.cn

Received 27.10.2019; accepted in revised form 05.03.2020

Abstract

The mold temperature of the downward continuous unidirectional solidification (CUS) cannot be controlled higher than the liquidus of alloys to be cast. Therefore, the continuous casting speed becomes the main parameter for controlling the growth of columnar crystal structure of the alloy. In this paper, the tin bronze alloy was prepared by the downward CUS process. The microstructure evolution of the CUS tin bronze alloy at different continuous casting speeds was analysed. In order to further explain the columnar crystal evolution, a relation between the growth rate of columnar crystal and the continuous casting speed during the CUS process was built. The results show that the CUS tin bronze alloy mainly consists of columnar crystals and equiaxed crystals when the casting speed is low. As the continuous casting speed increases, the equiaxed crystals begin to disappear. The diameter of the columnar crystal increases with the continuous casting speed increasing and the number of columnar crystal decreases. The growth rate of columnar crystal increases with increasing of the continuous casting speed during CUS tin bronze alloy process.

Keywords: Continuous unidirectional solidification, Tin bronze, Microstructure evolution, Continuous casting speed

1. Introduction

The continuous unidirectional solidification (CUS) process was used to prepare the high performance metals or alloys with columnar crystal or single crystal [1-4]. In order to obtaining the single crystal and columnar crystal, the key processing is to control the temperature gradient (G_L) in liquid phase at the front of solid–liquid interface and the growth rate (R) of crystal. In general, it is facilitate for the growth of columnar crystal or single crystal with the higher ratio of G_L/R [5]. During CUS process, the mold temperature needs to be heated above the liquidus temperature of the alloy so as to avoid the nucleation on the mold wall [6-9]. Therefore, the solid–liquid interface of the alloy is generally at the outer of the mold exit. However, for the downward CUS process, if the solid–liquid interface moves out of the mold exit, the molten metal may leak out of the mold, causing the experimental preparation to fail. So the solid–liquid interface is substantially maintained within the mold. In this case, the mold temperature may be lower than the liquidus of the alloy. There exist nuclei on the mold wall, and these nuclei furtherly develop into equiaxed crystals, which destroy the integrity of single crystal or columnar crystal. Therefore, in the case of mold temperature

decreasing, it is necessary to control the growth rate (R) of crystal for controlling the microstructure of the alloy.

On the other hand, Tin bronze alloys are widely used in semiconductor lead frames, cable connector relays, junction boxes and contact wires, etc[10-12]. During downward CUS tin bronze alloy process, low continuous casting speed will leads to serious exudation layer on the surface of the CUS tin bronze alloy [13]. In this work, downward CUS process was used to prepare tin bronze alloy. The mold temperature was controlled below the liquidus temperature of tin bronze alloy and different continuous casting speeds were chosen. The microstructure of the CUS tin bronze alloys was observed. Furthermore, the relation between the continuous casting speed and growth rate of columnar crystal was discussed.

2. Experimental

The material used for this experiment is tin bronze. The composition of the alloy can be seen in Table 1. The liquidus temperature of the alloy is about 1060 ℃.

Table 1.
Composition of tin bronze alloy

Element	Sn	Cu
Content (mass percentage)	3%	97%

The experiments were performed using the downward CUS method. Figure 1 shows the the diagram of downward CUS. The tin bronze alloy in the graphite crucible is melted by induction heating. The molten alloy flows into the graphite mold, which heated by the induction coil. Cooling water is provided at the exit of the mold to cool of solidified alloy. Starting the traction wheel, the alloy can be continuously pulled from the mold. Table 2 shows the experimental parameters.

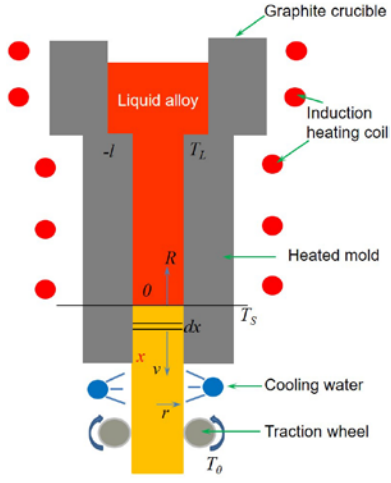

Fig. 1. Simplified sketch of the CUS process

Table 2.
Experimental parameters for CUS tin bronze alloys

Melt temperature (°C)	Mold temperature (°C)	Continuous casting speed (mm/min)	Cooling water temperature (°C)
1100	1050	4	25
1100	1050	8	25
1100	1050	12	25

Samples were cut from the CUS tin bronze alloys for optical microscopy analysis. After polishing, the samples were etched by ferric nitrate solution. The microstructure observation was performed by using Nikon Coolpix 995 optical microscope.

3. Results and Discussion

3.1. Microstructures of CUS tin bronze

Figure 2 shows the microstructure of CUS tin bronze alloys under different continuous casting speeds. While the continuous casting speed is 4 mm/min, the microstructure mainly consists of columnar crystals and equiaxed crystals, as shown in Figure 2(a). It can be found that there exist both the columnar crystals and the equiaxed crystals and the integrity of columnar crystals is destroyed by equiaxed crystals. On one hand, temperature gradient between melt and solidified alloy is established due to the intense cooling near the mold exit. Therefore, there exists a heat flow parallel to the casting direction. The crystals grow in the opposite direction of the temperature gradient to form columnar crystals. On the other hand, since the temperature of the mold is below the liquidus, crystals nucleate on the mold wall and grow up, and drop in front of the solid–liquid interface induced by thermal convection to form the equiaxed crystals.

While the continuous casting speed is increased to 8 mm/min, it can be seen that there are four columnar crystals and the equiaxed crystals disappear, as shown in Figure 2(b). The average diameter of columnar crystal is about 900 μm. While the continuous casting speed reaches to 12 mm/min, the average diameter of columnar crystal is increase to about 1200 μm, as shown in Figure 2(c). As the continuous casting speed increases, the growth rate of the crystal begins to increase. During the growth of the columnar crystals, the faster growing columnar crystals gradually eliminate the slower growing ones. As a result, the number of columnar crystals begins to decrease and the diameter of the columnar crystals begins to increase.

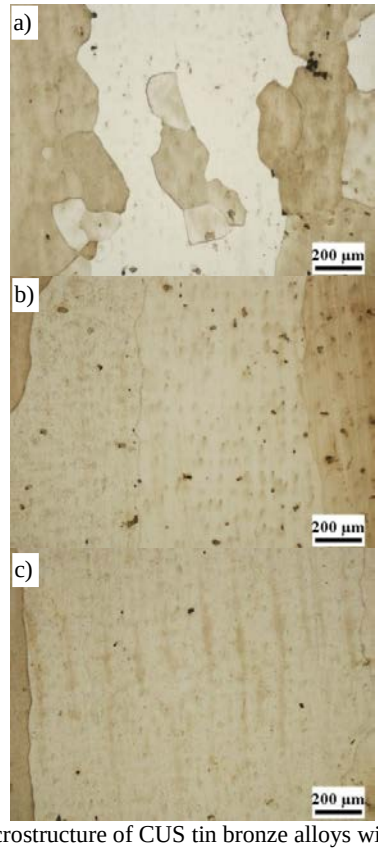

Fig. 2. Microstructure of CUS tin bronze alloys with different continuous casting speed, a) 4 mm/min, b) 8 mm/min, c) 12 mm/min.

3.2. Relation between the continuous casting speed and crystal growth rate

In order to establish the relation between the continuous casting speed and the growth rate of columnar crystal, an analysis and discussion of the heat transfer process in heated mold is performed. The following assumptions are established:

1) The influence of convection and radiation of the molten metal on the mold temperature is not considered.
2) The heat transfer from the system to the surroundings is performed by solidified metal that forced cooling through water spray.
3) The temperature at the mold entrance stays the same.

The coordinate is selected at the solid–liquid interface, as shown in Figure 1. Consider a cylindrical element in the solid crystal *dx* in thickness, moving with the speeding of *v* (continuous casting speed). The distance between the element and the solid–liquid interface is kept constant. Then, the heat balance equation of the moving element is written [14].

Heat change from conduction + Heat change from boundary movement + Heat change from loss to surroundings = 0

$$\alpha_s \frac{d^2T}{dx^2}\left(\rho_s c_s \pi r^2 dx\right) - v\frac{dT}{dx}\left(\rho_s c_s \pi r^2 dx\right) - h\left(T - T_0\right)\left(2\pi r^2 dx\right) = 0 \tag{1}$$

Where, α_s is thermal diffusivity of the solid crystal, ρ_s is density of the solid crystal, v is the continuous casting speed, h is heat transfer coefficient for heat loss to surrounding, c_s is specific heat of solid metal, T is temperature, T_0 is ambient temperature, r is radius of the alloy.

From the boundary conditions, while x=0, T=T_S, and x=∞, T=T_0, the temperature of solidified alloy can be obtained from the following equation:

$$\frac{T - T_0}{T_S - T_0} = \exp\left\{-\left[\frac{v}{2\alpha_s} - \sqrt{\left(\frac{v}{2\alpha_s}\right)^2 + \frac{2h}{rK_S}}\right]x\right\} \tag{2}$$

Where, T_S is solidus temperature, *Ks* is thermal conductivity of solid metal.

The temperature gradient (G_S) of the solid at the liquid–solid interface is

$$G_S = \left(\frac{dT}{dx}\right)_{x=0} \tag{3}$$

Derivation of Equation 3 shows

$$G_s = -\left(T_S - T_0\right)\left[\frac{v}{2\alpha_s} - \sqrt{\left(\frac{v}{2\alpha_s}\right)^2 + \frac{2h}{rK_s}}\right] \tag{4}$$

Similarly, the heat balance equation in the solid–liquid two-phase region is

$$\lambda\left(\frac{\partial^2 T}{\partial x^2}\left(\rho_{L\text{-}S} c_{L\text{-}S} \pi r^2 dx\right) + \frac{\partial^2 T}{\partial y^2}\left(\rho_{L\text{-}S} c_{L\text{-}S} \pi r^2 dx\right)\right) - v\frac{\partial T}{\partial x}\left(\rho_{L\text{-}S} c_{L\text{-}S} \pi r^2 dx\right) = 0 \tag{5}$$

Where, λ is thermal conductivity of alloy, $\rho_{L\text{-}S}$ is density of the alloy in solid–liquid two-phase region, $c_{L\text{-}S}$ is specific heat of metal in solid–liquid two-phase region. Equation 5 can be simplified as

$$\lambda\left(\frac{\partial^2 T}{\partial x^2} + \frac{\partial^2 T}{\partial y^2}\right) - v\frac{\partial T}{\partial x} = 0 \tag{6}$$

Because analysis of the above two-dimensional partial differential equations is tedious, the heat transfer equation will be calculated respectively in the axial and radial directions.

$$\begin{cases} \lambda\dfrac{d^2T}{dx^2} - v\dfrac{dT}{dx} = 0 \\ \lambda\dfrac{d^2T}{dy^2} = 0 \end{cases} \tag{7}$$

Using $T=T(x)T(y)$ to approximate the temperature, then

$$T = T(x)^2 + \frac{T_L l - (T_L - T_S)x}{rl} T(x) \tag{8}$$

Where, T_L is liquidus temperature, l is length of heated mold.

The temperature gradient of the liquid (G_L) at the liquid–solid interface is given by

$$G_L = \left(\frac{dT}{dx}\right)_{x=0} \tag{9}$$

Derivation of Equation 9 shows

$$G_L = (T_L - T_S)\left[\frac{\frac{v}{\lambda}\left(T_S - \frac{T_L}{r}\right)}{\left(\exp\left(-\frac{v}{\lambda}\right)-1\right)} - \frac{T_S}{rl}\right] \tag{10}$$

Assuming that latent heat is released at x=0, the heat balance at the solid–liquid interface during solidification is [11]

$$K_S G_S - K_L G_L = \rho_S H R \tag{11}$$

Where, K_L is thermal conductivity of liquid metal, R is growth rate of columnar crystal, H is heat of fusion. Substituting Equation 4 and Equation 10 into Equation 11, the growth rate of columnar crystal R is given by

$$R = -\frac{1}{\rho_S H}\left\{(T_S - T_0)\left[\frac{v}{2\alpha_s} - \sqrt{\left(\frac{v}{2\alpha_s}\right)^2 + \frac{2h}{rK_S}}\right]K_S + (T_L - T_S)\left[\frac{\frac{v}{\lambda}\left(T_S - \frac{T_L}{r}\right)}{\left(\exp\left(-\frac{v}{\lambda}\right)-1\right)} - \frac{T_S}{rl}\right]K_L\right\} \tag{12}$$

Equation 12 is the relation between the growth rate of the columnar crystal (R) and the continuous casting speed (v). The minus in the front indicates that the growth direction of columnar crystals is opposite to the continuous casting speed. It can be seen from the Equation 12 that while the continuous casting speed (v) is increasing, the growth rate of columnar crystal (R) is also increases at the same time.

In this experiment, since the temperature of the alloy in the mold is controlled at 1050 ℃ during the CUS process, which is lower than that of the liquidus of the tin bronze alloy. While the continuous casting speed is low (4 mm/min), according to Equation 12, the growth rate of the columnar crystal is also slower. Meanwhile, there exists nucleation on the mold wall, and gradually develops into equiaxed crystal. The upwardly growing columnar crystal and the equiaxed crystal come into contact with each other, finally forming a coexisting microstructure of columnar crystal and equiaxed crystal. As the continuous casting speed increase (8 mm/min and 12 mm/min), the growth rate of the columnar crystal starts to increase. Because the columnar crystal rapidly grow upwards to liquid of alloy, the equiaxed crystal is too late to grow. Second, as the casting speed increases, liquid metal with higher temperature in the crucible quickly flows downward into the mold. Thus leading to the temperature of the alloy in the mold is high, which inhibits the occurrence of nucleation on the mold wall. Therefore, there is no equiaxed crystal can be found in CUS tin bronze alloys with high speed of 8 mm/min and 12 mm/min. When the continuous casting speed is further increased, the columnar crystal rapidly grows upwards. However, the columnar crystal with slower growth rate is gradually eliminated, thereby forming coarse columnar crystal.

4. Conclusions

In summary, Tin bronze alloys were prepared by the downward CUS process. With the continuous casting speed increase, columnar crystals gradually replace equiaxed crystals as the main component of the CUS tin bronze alloy. The diameter of the columnar crystals also begins to increase when the continuous casting speed is further increasing. The relation between the growth rate of columnar crystals and the continuous casting speed is built.

References

[1] Okayasu, M. & Takeuchi, S. (2017). Mechanical properties of cast Al–Mg_5 alloy produced by heated mold continuous casting. *International Journal of Metalcasting.* 12(2), 298-306. DOI: 10.1007/s40962-017-0163-6.

[2] Soda, H., McLean, A., Wang, Z. & Motoyasu, G. (1995). Pilot-scale casting of single-crystal copper wires by the Ohno continuous casting process. *Journal of Materials Science*. 30, 5438-5448. DOI: 10.1007/BF00351555.

[3] Wang, Y.H., Xiao, L.R., Zhao, X.J., Hu, W., Song, Y.F., Zhang, W. & Zhou, H. (2015). Microstructure and mechanical properties of columnar-grained copper produced by the Ohno continuous casting technique. *Materials Science and Engineering: A.* 639, 122-130. DOI: 10.1016/j.msea.2015.04.099.

[4] Yang, F., Wang, J., Yu, J., Zhou, Z., Wang, B., Tu, T., Ren X., Deng, K. & Ren, Z. (2019). Microstructure and mechanical properties of Ni-based superalloy K418 produced by the continuous unidirectional solidification process. *Journal of Materials Engineering and Performance.* 28(10), 6483-6491. DOI: 10.1007/s11665-019-04385-5.

[5] Flemings, M.C. (1974). Solidification processing. *Metallurgical Transactions.* 5, 2121-2134. DOI: 10.1007/bf02643923.

[6] Luo, J.H. (2018). Formation mechanism of surface segregation in heated mold continuous casting Al–Cu Alloy. *Light Metals 2018*. 435-439. DOI: 10.1007/978-3-319-72284-9_59.

[7] Okayasu, M., Takeuchi, S., Wu, S. & Ochi, T. (2016). Effects of Sb, Sr, and Bi on the material properties of cast Al Si–Cu alloys produced through heated mold continuous casting. *Journal of Mechanical Science and Technology*. 30(3), 1139-1147. DOI: 10.1007/s12206-016-0218-2.

[8] Ohno, A. (1986). Continuous casting of single crystal ingots by the O.C.C process. *JOM*. 38(1), 14-16. DOI: 10.1007/BF03257948.
[9] Okayasu, M., Takasu, S. & Yoshie, S. (2010). Microstructure and material properties of an Al–Cu alloy provided by the Ohno continuous casting technique. *Journal of Materials Processing Technology*. 210, 1529-1535. DOI: 10.1016/j.jmatprotec.2010.04.012.
[10] Al-Ganainy, G.S., Fawzy, A. & El-Salam, F. (2004). Transient and steady-state creep characteristics of Cu−2wt%Sn alloy in the solid solution region. *Physica B*: *Comdensed Matter*. 344(1-4), 443-450. DOI: 10.1016/ j.physb.2003.10.028.
[11] Song, J.Y., Yu, J. & Lee, T.Y. (2004). Effects of reactive diffusion on stress evolution in Cu−Sn films. *Scripta Materialia*. 51(2), 167-170. DOI: 10.1016/j.scriptamat. 2004.03.032.
[12] Debiemme-Chouvy, C., Ammeloot, F. & Sutter, E.M.M. (2001). X-ray photoemission investigation of the corrosion film formed on a polished Cu−13Sn alloy in aerated NaCl solution. *Applied Surface Science*. 174(1), 55-61. DOI: 10.1016/s0169-4332(01)00023-x.
[13] Luo, J.H. & He, F. (2019). Effect of process parameters on exudation thickness in continuous unidirectional solidification tin bronze alloy. *Archives of Foundry Engineering*. 19(2), 97-100. DOI: 10.24425/afe. 2019.127123.
[14] Flemings, M.C. (1974). *Solidification Processing*. New York: McGrall Hill.